Molecular Therapy
Methods & Clinical Development
Original Article

AAV-mediated inner ear gene delivery triggers mild host immune responses in the mammalian inner ear

Yasuko Ishibashi,[1,2] Jianliang Zhu,[1] Gwladys Gernoux,[3] Yunkai Yu,[4] Michelle J. Suh,[1] Kevin Isgrig,[1] Mhamed Grati,[1] Rafal Olszewski,[5] Michael Hoa,[5] Cao Liang,[4] Thomas B. Friedman,[2] Oumeya Adjali,[3] and Wade W. Chien[1,6]

[1]Inner Ear Gene Therapy Program, National Institute on Deafness and Other Communication Disorders, National Institutes of Health, Bethesda, MD 20892, USA; [2]Laboratory of Molecular Genetics, National Institute on Deafness and Other Communication Disorders, National Institutes of Health, Bethesda, MD 20892, USA; [3]Nantes Université, CHU de Nantes, INSERM, TaRGeT - Translational Research in Gene Therapy, UMR 1089, F-44200 Nantes, France; [4]OMICS Technology Facility, Genetics Branch, The Center for Cancer Research, National Cancer Institute, National Institutes of Health, Bethesda, MD 20892, USA; [5]Auditory Development and Restoration Program, National Institute on Deafness and Other Communication Disorders, National Institutes of Health, Bethesda, MD 20892, USA; [6]Department of Otolaryngology-Head and Neck Surgery, Johns Hopkins School of Medicine, Baltimore, MD, USA

Hearing loss is a common disability affecting the world's population. Currently, its treatment options are limited. Adeno-associated virus (AAV)-mediated inner ear gene therapy has shown great promise as a treatment for hereditary hearing loss. However, the host immune responses to AAV-mediated gene therapy in the mammalian inner ear is not well understood. In this study, two serotypes of AAV vectors were injected individually into the mouse inner ear to evaluate the host innate and adaptive immune responses up to 1 month after inner ear gene delivery. Our results suggest that the host innate and adaptive immune responses to AAV-mediated inner ear gene delivery are limited and mild, which is favorable for its clinical translation.

INTRODUCTION

The mammalian inner ear is a promising target for gene therapy because it is relatively isolated anatomically. The inner ear is housed in the otic capsule of the temporal bone, which is one of the densest bones in the body, and it is protected by the blood-labyrinth barrier, blood-strial barrier, and the blood-perilymph barrier.[1] The structural and physiological uniqueness of the inner ear allows for targeted viral transduction. Adeno-associated virus (AAV) belongs to the family *Parvoviridae*.[2] It is a non-enveloped virus with a single-stranded DNA genome. AAV is among the most frequently used viral vectors in human gene therapy clinical trials due to its high transduction efficiency, the ability to engineer various viral capsids to target different cell types,[3] and its documented safety profile.[4] For the inner ear, multiple proof-of-concept studies have shown that gene therapy is effective at improving the auditory and vestibular functions in animal models of hereditary hearing loss,[5] and recent clinical trials have shown encouraging responses.[6–8] Despite the advantageous features of AAV as a gene therapy viral vector, it has been reported that AAV can trigger host immune responses in clinical trials targeting other organs.[9–11] This could have a significant impact on the efficacy of the gene therapy and may cause morbidities in patients.[9,12–14] Thus, it is critical to investigate the host immune responses in the setting of AAV-mediated inner ear gene therapy to maximize its therapeutic potential and to ensure patient safety.

The host immune responses to foreign pathogens are categorized into innate and adaptive immunity.[15,16] The innate immune responses occur within several hours after exposure to pathogens and are relatively non-specific. The cellular component of the innate immune responses is initiated by a subset of leukocytes, such as neutrophils, macrophages, monocytes, and natural killer (NK) cells.[15] The complement system mediates the humoral component of the innate immune responses and induces the release of pro-inflammatory cytokines. It also serves as a bridge to the adaptive immune responses.[16,17] In contrast, the adaptive immune responses are usually initiated several days after the initial exposure to pathogens and are mediated by antigen-specific B cells and T cells with long-lasting immunological memories.[16] In this study, we administered two serotypes of AAV vectors individually through the posterior semicircular canal (PSCC) approach into the inner ears of adult mice.[18] The innate and adaptive immune responses against AAV-mediated gene delivery were investigated both locally and systemically.

RESULTS

AAV-mediated inner ear gene delivery activates macrophages in the cochlea

CX3CR1 is a membrane receptor for fractalkine, also known as CX3CL1. Fractalkine plays important roles in the immune responses

Received 10 September 2024; accepted 18 March 2025;
https://doi.org/10.1016/j.omtm.2025.101456.

Correspondence: Wade W. Chien, Inner Ear Gene Therapy Program, National Institute on Deafness and Other Communication Disorders, National Institutes of Health, Bethesda, MD 20892, USA.
E-mail: wade.chien@nih.gov

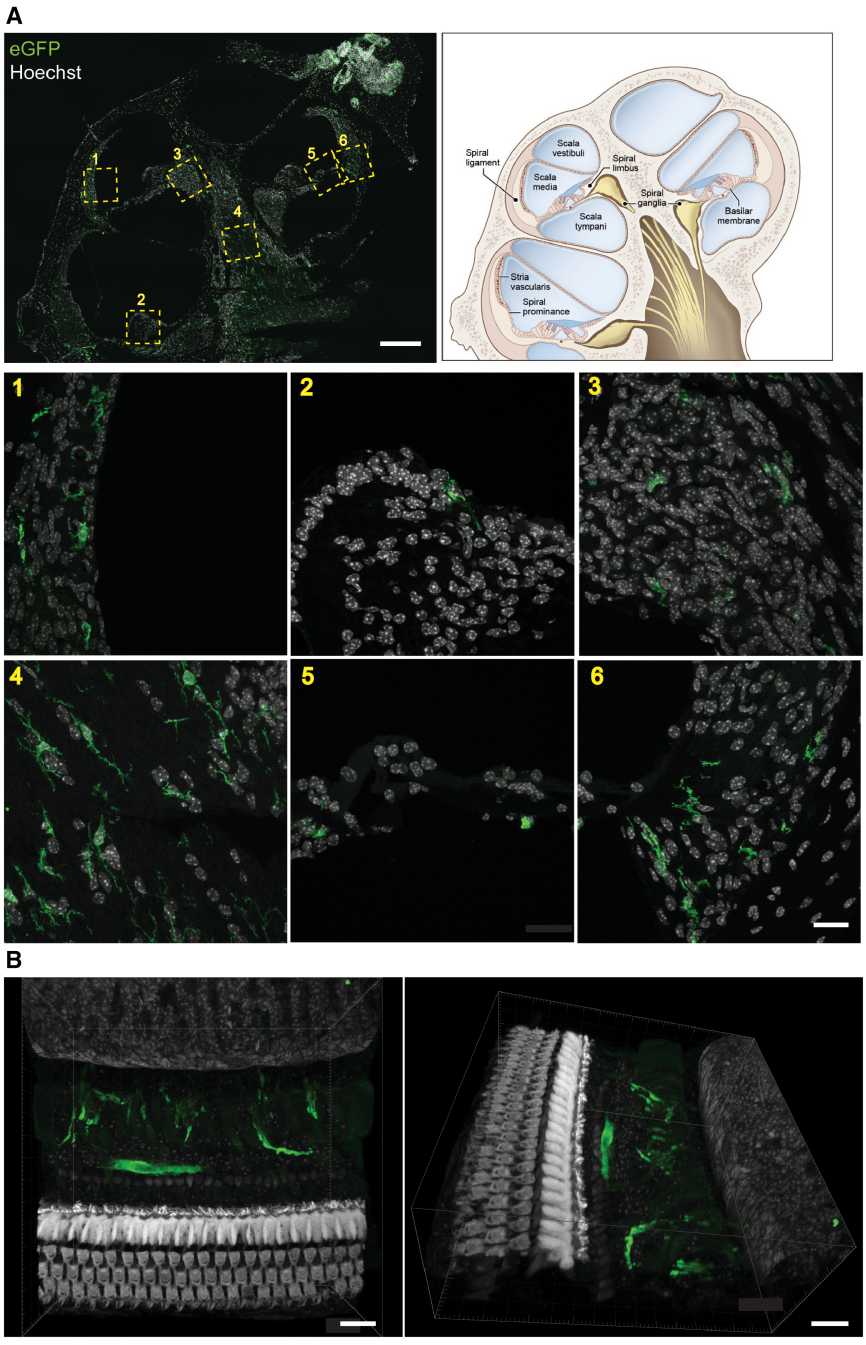

Figure 1. Localization of resident macrophages in the mouse cochlea

Cx3cr1$^{GFP/GFP}$ mice are used to localize resident macrophages in cochlea. (A) A mid-modiolar cross-sectional image of the cochlea from a non-surgery *Cx3cr1*$^{GFP/GFP}$ mouse is shown, along with a cartoon illustration. Scale bar, 200 μm. Magnified images from various regions of the cochlea with macrophages are shown: stria vascularis (1), spiral limbus (2), Rosenthal's canal (3), modiolus (4), basilar membrane and osseus lamina (5), and spiral prominence (6). Scale bar, 20 μm. (B) Three-dimensional reconstruction images of the cochlear middle turn from a non-surgery *Cx3cr1*$^{GFP/GFP}$ mouse are shown, viewing the cochlea from two different directions. Macrophages are observed along the basilar membrane to the osseus spiral lamina. Scale bars, 20 μm.

and neural protection.[19] The *Cx3cr1*$^{GFP/GFP}$ mouse replaces *Cx3cr1* with eGFP and labels various immune cells with eGFP, such as monocytes, macrophage, dendritic cells, microglia, and NK cells.[20–28] Multiple studies have examined the localization of macrophages in the inner ear using this mouse strain.[20–28] Under normal conditions in the mature cochlea, macrophages are found in the cochlear lateral wall, spiral limbus, Rosenthal's canal, modiolus, basilar membrane, osseous spiral lamina, and spiral prominence (Figure 1).[20] These resident macrophages play important roles in maintaining the homeostasis of the inner ear.[29] They also help to mediate innate immune responses when the inner ear is first exposed to pathogens or cell injuries.[20,30] Thus, the *Cx3cr1*$^{GFP/GFP}$ mouse provides a good model for tracking innate immune responses following AAV-mediated gene delivery into the inner ear.

To study the innate immune response to AAV-mediated inner ear gene delivery, AAV2.7m8-CAG-tdTomato (1.1×10^{10} GC) was injected into the PSCC of 8- to 10-week-old *Cx3cr1*$^{GFP/GFP}$ mice. The hair cell transduction rates of *Cx3cr1*$^{GFP/GFP}$ mice injected with AAV2.7m8-CAG-tdTomato were evaluated to confirm viral transduction (n = 4, female = 2, male = 2) (Table S1). The transduction rate (mean ± SD) of inner hair cells (IHCs) was 78.74 ± 5.47% in the apex, 90.10 ± 1.99% in the middle turn, and 66.21 ± 23.07% in the basal turn. Transduction rate of outer hair cells was 9.63 ± 1.75% in the apex, 9.84 ± 1.40% in the middle turn, and 2.75 ± 3.38% in the basal turn. The cochleae of the injected mice were harvested on post-operative day (POD) 1, 3, 7, 14, 21, and 28. Age-matched non-injected *Cx3cr1*$^{GFP/GFP}$ mice were used as negative controls. Representative images in each group were presented in Figure 2. On POD1, the number of macrophages labeled by eGFP in the cochlea did not increase significantly compared with non-surgery controls. Anti-CD68 antibody, a pan-macrophage marker,[31] was also used to label the macrophages to confirm their identity (Figures 2A and 2B). However, by POD3, an increase in eGFP was observed in the injected cochleae, indicating an increase in macrophages (Figure 2C).

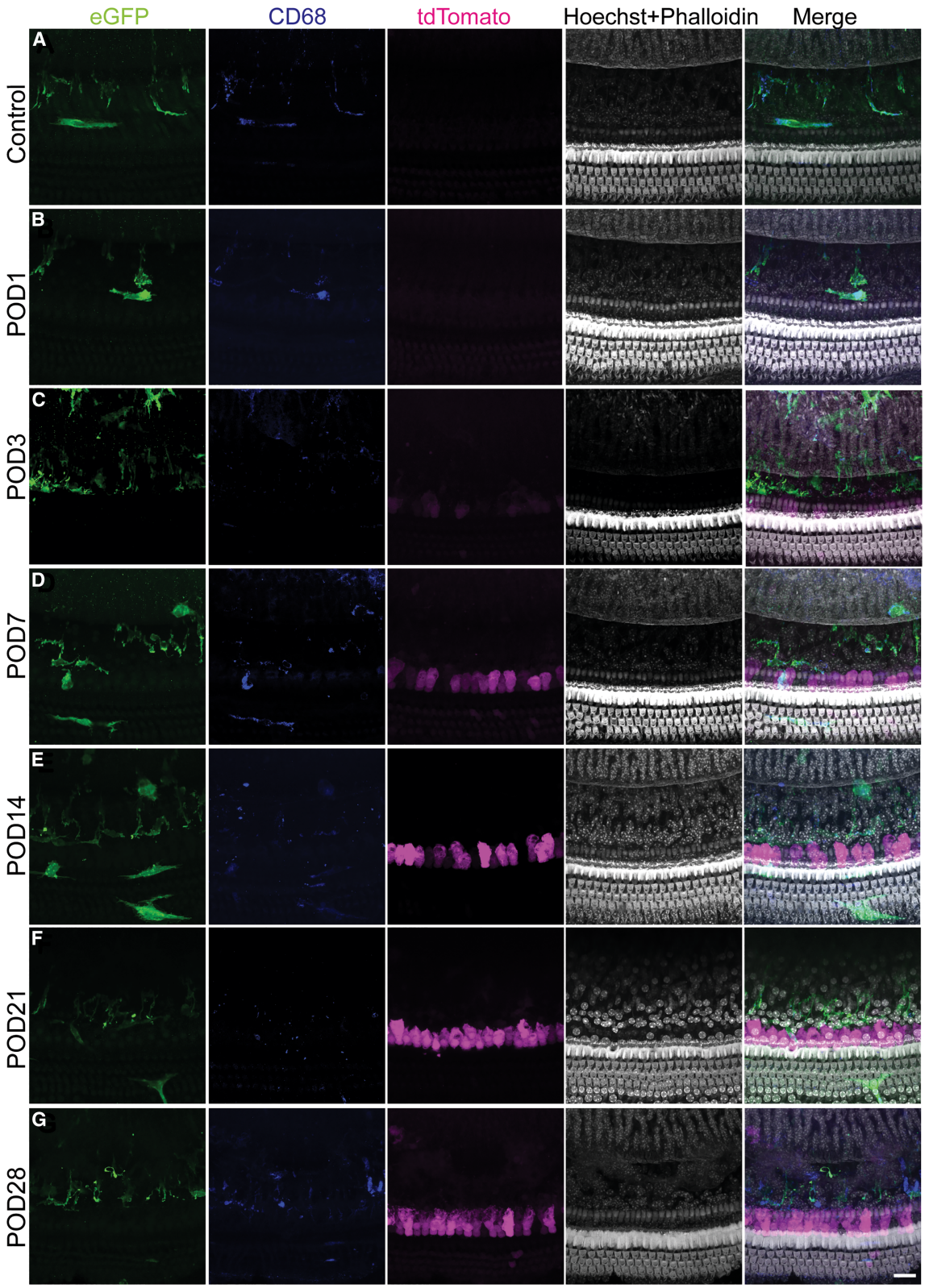

(legend on next page)

Of note, AAV2.7m8-tdTomato transgene expression was first observed on POD3. On POD7, macrophages were observed along the basilar membrane that is located under the organ of Corti (Figure 2D). The number of macrophages in the injected cochleae continued to increase up to POD14 (Figure 2E). By POD21, the number of macrophages declined, even though the number of transduced IHCs increased (Figure 2F). By POD28, the number of macrophages returned to baseline (Figure 2G). We repeated this experiment with AAV2-CAG-tdTomato (1.0×10^{10} GC) and observed similar trends (Figure S1).

AAV-mediated inner ear gene delivery triggers an increase in macrophages but not T cells in the cochlea

The *Cx3cr1*$^{GFP/GFP}$ mouse strain allowed us to trace the macrophages in the inner ear. However, since the CX3CR1 receptor plays critical roles in immune responses, immune-neural communications,[32] and neural protections,[33–35] it is possible that the *Cx3cr1*$^{GFP/GFP}$ mouse, which replaces *Cx3cr1* with sequence encoding eGFP, may have ameliorated immune responses.[20,36] Therefore, we also assessed macrophage activation in the cochlea after AAV-mediated inner ear gene delivery using the C57BL/6 mice. Eight- to 10-week-old C57BL/6 mice were injected unilaterally with either AAV2.7m8-CAG-eGFP (1.0×10^{10} GC), AAV2-CAG-eGFP (1.0×10^{10} GC), or viral storage buffer (1× PBS and 5% glycerol, termed vehicle) via the PSCC approach. To confirm appropriate AAV-mediated gene delivery to the inner ear, we assessed the viral transduction on POD28 by quantifying eGFP expression in the cochlea. The average IHC transduction rates (mean ± SD) in the cochlea were 84.65 ± 16.50% for AAV2.7m8-CAG-eGFP and 64.57 ± 25.21% for AAV2-CAG-eGFP. Specific transduction rates for each cochlear turn are presented in Table S2. These transduction rates were consistent with a previous study.[18] Macrophages were labeled using an antibody targeting the ionized calcium-binding adapter molecule 1 (IBA1).[29] We found that macrophages were localized in similar locations in the cochleae of adult non-surgery C57BL/6 mice compared with *Cx3cr1*$^{GFP/GFP}$ mice (Figure S2). Additionally, we used the anti-CD3 antibody as a marker for T cells. T cells were barely detectable in non-injected mice. To quantify the changes in the number of macrophages and T cells after AAV-mediated gene delivery, the treated cochleae were harvested at POD3 and POD28. POD3 was chosen to detect the innate immune responses, which is typically triggered within 4 days after pathogen exposure.[15] The cochleae from age-matched non-surgery mice were used as negative controls. POD28 was selected as the approximate time point when maximal viral transduction was expected.[37] The eGFP signals were detectable by POD3 and increased by POD28 for both AAV2.7m8 and AAV2-CAG-eGFP-injected mice (Figure S3). Whole-mount images from the sensory epithelium (Figure 3C) and lateral wall (Figure 3F) were used for quantification of macrophages and T cells in the cochlea. The number of animals used and the respective p values are summarized in Table 1. In the sensory epithelium, an increase in cochlear macrophages was observed in all injected mice on POD3 compared with non-surgery control mice (Figure 3A). The increase in macrophages was statistically significant in vehicle-injected mice compared with non-surgery control mice in the apical and middle turns ($p = 0.019$ for apical turn and $p = 0.014$ for the middle turn, Kruskal-Wallis test with Dunn's multiple comparisons). In the lateral wall on POD3, we also observed an increase in cochlear macrophages in all injected mice compared with non-surgery control mice (Figure 3D). The increase in macrophages was statistically significant in AAV2-injected mice compared with non-surgery control mice in the middle and basal turns ($p = 0.044$ for both the middle and basal turns, Kruskal-Wallis test with Dunn's multiple comparisons). The fact that similar levels of increases in cochlear macrophages were observed in mice injected with AAV and vehicle suggests that the increase in macrophages on POD3 may be due to surgical trauma, and not due to AAV-mediated gene delivery alone. On POD28, we did not observe any statistically significant increases in the number of macrophages in all cochlear turns compared with non-surgery control mice both in the sensory epithelium (Figure 3B) and in the lateral wall (Figure 3E). Interestingly, there was no statistically significant increase in the number of T cells between AAV2.7m8-injected, AAV2-injected, or vehicle-injected mice compared with non-surgery mice at POD3 and POD 28, both in the sensory epithelium and in the lateral wall (Figure 3). We also did not observe any increase in macrophages or T cells in the utricles between AAV2.7m8-injected, AAV2-injected, or vehicle-injected mice compared with non-surgery mice at POD3 and POD 28 (Figures 3G and 3H). These results suggest that, while macrophages were recruited to the cochlea, the number of T cells did not increase significantly within 28 days after AAV-mediated inner ear gene delivery.

AAV-mediated inner ear gene delivery triggers neutralizing antibody production

An essential aspect of the adaptive immune response is the production of antibodies mediated by B cells. We examined whether AAV-mediated inner ear gene delivery would result in the production of neutralizing antibodies in the serum. Adult C57BL/6 mice (8–10 weeks old) were injected either with AAV2.7m8-CAG-eGFP (1.0×10^{10} GC), AAV2-CAG-eGFP (1.0×10^{10} GC), or vehicle, and the serum was collected at POD28 for analyses (Figure 4). The serum from mice that were injected with vehicle had a mean neutralizing antibody titer of 28.01 ± 51.46 (mean ± SD) against AAV2-CAG-eGFP ($n = 8$, female = 4, male = 4). The serum of AAV2-CAG-eGFP-injected mice had a mean neutralizing antibody titer of 3,535.59 ± 3,795.54 against AAV2-CAG-eGFP ($n = 7$, female = 4, male = 3). This was statistically

Figure 2. Macrophage activation after AAV2.7m8-mediated inner ear gene delivery in *Cx3cr1*$^{GFP/GFP}$ mice

Confocal images of the *Cx3cr1*$^{GFP/GFP}$ cochlear middle turns are shown. Adult (8- to 10-week-old) *Cx3cr1*$^{GFP/GFP}$ mice underwent AAV2.7m8-CAG-tdTomato injections via the PSCC approach, and cochleae were processed on POD 1, 3, 7, 14, 21, 28 (B–G). Cochlear images from a non-surgery *Cx3cr1*$^{GFP/GFP}$ mouse are shown for comparison (A). The eGFP (green) and CD68 (blue) antibodies are used to label macrophages, tdTomato (magenta) expression indicates viral transduction, and Hoechst and phalloidin stains (white) label the nucleus and F-actin, respectively. Scale bar, 20 μm.

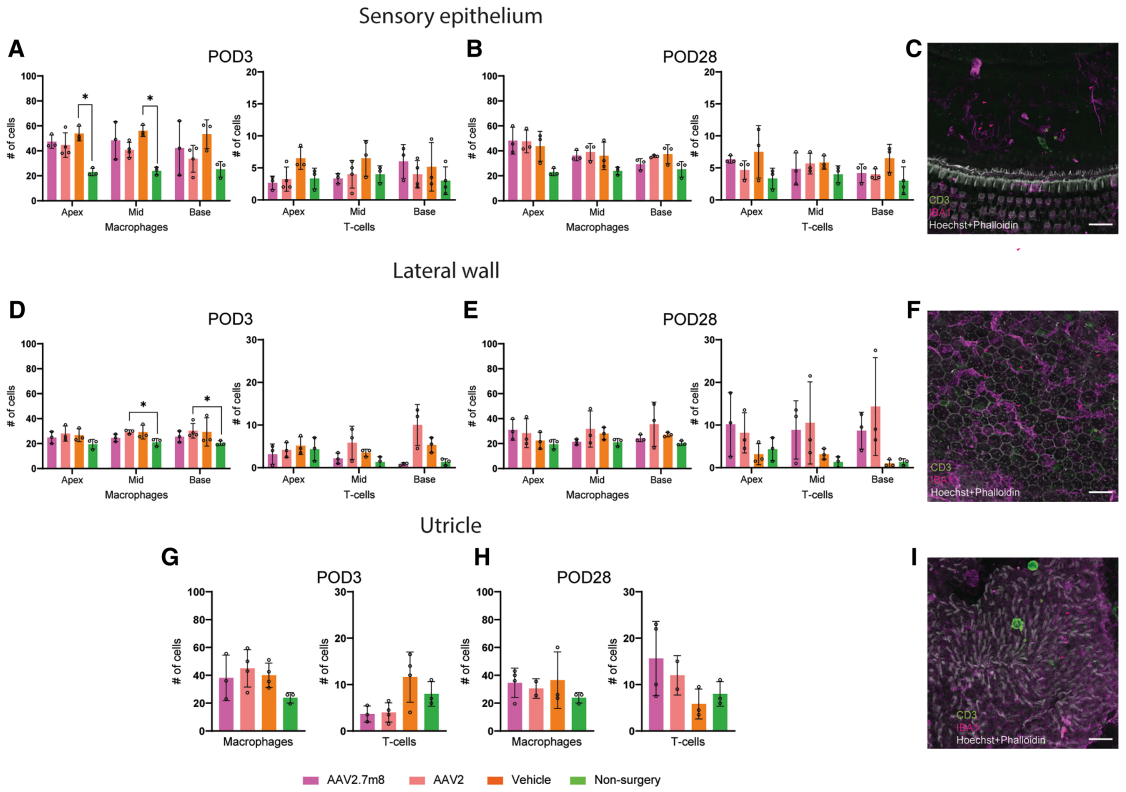

Figure 3. Macrophage and T cell activation after AAV-mediated inner ear gene delivery in C57BL/6 mice

C57BL/6 mice were used to localize the macrophages and T cells in the cochlea and utricle after AAV-mediated inner ear gene delivery. Quantification of macrophages (by anti-IBA1 antibody) and T cells (by anti-CD3 antibody) were done using whole-mount images of the sensory epithelium (A and B), lateral wall (C and D), and utricle (G and H). Quantifications were performed on POD3 and POD28. Sample whole-mount images used for quantification are shown (C, sensory epithelium; F, lateral wall; I, utricle). Animals that did not undergo surgery were used as non-surgery controls. The scale bars represent 20 μm. Kruskal-Wallis test with Dunn's multiple comparisons were used for statistical analysis. *$p < 0.05$.

significantly higher than the mean neutralizing antibody titer of the vehicle-injected group ($p = 0.0077$, Kruskal-Wallis test with Dunn's multiple comparisons). The serum of AAV2.7m8-CAG-eGFP-injected mice had a mean neutralizing antibody titer of 11,156.05 ± 7,567.70 against AAV2.7m8-CAG-eGFP ($n = 8$, female = 4, male = 4). This was significantly higher than the mean neutralizing antibody titer in vehicle-injected mice ($p < 0.0001$, Kruskal-Wallis test with Dunn's multiple comparisons). We also tested the cross-reactivity of the serum of AAV2-CAG-eGFP-injected mice against AAV2.7m8 vector and found that the mean neutralizing antibody titer was 181.93 ± 77.32 ($n = 3$, female = 1 and male = 2, $p > 0.99$, Kruskal-Wallis test with Dunn's multiple comparisons). On the other hand, the serum of AAV2.7m8-CAG-eGFP-injected mice had a mean neutralizing antibody titer of 1,220.17 ± 784.80 against AAV2-CAG-eGFP ($n = 3$, female = 2 and male = 1, $p = 0.82$, Kruskal-Wallis test with Dunn's multiple comparisons). Our results indicated that AAV-mediated inner ear gene delivery triggered the humoral component of the adaptive immune response in the serum for both AAV2 and AAV2.7m8 within 1 month from surgery.

AAV-mediated inner ear gene delivery does not trigger an interferon-γ-mediated peripheral cellular immune response

In addition to B cells, T cells also play an important role in mediating the adaptive immune responses. In fact, exposure to foreign antigens such as AAV can trigger the release of the inflammatory cytokine interferon gamma (IFN-γ). To assess whether AAV-mediated inner ear gene delivery triggers an antigen-specific IFN-γ-mediated T cell response, splenocytes from mice injected with AAV2.7m8-CAG-eGFP (1.0×10^{10} GC, $n = 7$, female = 6, male = 1), AAV2-CAG-eGFP (1.0×10^{10} GC, $n = 7$, female = 5, male = 2), or vehicle ($n = 8$, female = 2, male = 6) were harvested. All samples were analyzed on POD28 using an IFN-γ ELISpot assay. The splenocytes were stimulated *in vitro* with an overlapping peptide library spanning the VP1 sequence from AAV2.7m8 or AAV2, and the peptides were divided into three pools (VP1a, VP1b, and VP1c). Unstimulated cells (culture media only) were used as a negative control, and concanavalin A stimulation was used as a positive control for cytokine secretion. Of the seven mice that were injected with AAV2.7m8-CAG-eGFP, six mice did not show an IFN-γ-positive

Table 1. Summary of the number of mice and *p* values for activation of macrophages and T cells following AAV-mediated inner ear gene delivery in adult C57BL/6 mice

		POD3			POD28		
		Apical turn	Middle turn	Basal turn	Apical turn	Middle turn	Basal turn
Macrophages							
Sensory epithelium	AAV2.7m8-CAG-eGFP-injected POD3 $n = 3$ (f = 2,m = 1), POD28 $n = 3$ (f = 1,m = 2)	0.11	0.11	0.31	0.09	0.12	>0.99
	AAV2-CAG-eGFP-injected POD3 $n = 4$ (f = 2,m = 2), POD28 $n = 3$ (f = 1,m = 2)	0.33	0.39	0.92	0.12	0.70	0.14
	vehicle-injected POD3 $n = 3$ (f = 2,m = 1), POD28 $n = 3$ (f = 1,m = 2)	0.019[a]	0.014[a]	0.11	0.16	0.21	0.16
Lateral wall	AAV2.7m8-CAG-eGFP-injected POD3 $n = 3$ (f = 2,m = 1), POD28 $n = 3$ (f = 2,m = 1)	0.52	>0.99	0.47	0.18	>0.99	0.77
	AAV2-CAG-eGFP-injected POD3 $n = 3$ (f = 2,m = 1), POD28 $n = 3$ (f = 2,m = 1)	0.09	0.044[a]	0.044[a]	0.63	0.58	0.30
	vehicle-injected POD3 $n = 3$ (f = 2,m = 1), POD28 $n = 3$ (f = 1,m = 2)	0.27	0.16	0.28	>0.99	0.27	0.24
Utricle	AAV2.7m8-CAG-eGFP-injected POD3 $n = 3$ (f = 2,m = 1), POD28 $n = 4$ (f = 2,m = 2)	0.43			0.65		
	AAV2-CAG-eGFP-injected POD3 $n = 4$ (f = 2,m = 2), POD28 $n = 4$ (f = 2,m = 2)	0.065			>0.99		
	vehicle-injected POD3 $n = 4$ (f = 2,m = 2), POD28 $n = 3$ (m = 3)	0.20			>0.99		
T cells							
Sensory epithelium	AAV2.7m8-CAG-eGFP-injected POD3 $n = 3$ (f = 2,m = 1), POD28 $n = 3$ (f = 1,m = 2)	>0.99	>0.99	0.25	0.16	>0.99	>0.99
	AAV2-CAG-eGFP-injected POD3 $n = 4$ (f = 2,m = 2), POD28 $n = 3$ (f = 1,m = 2)	>0.99	>0.99	>0.99	>0.99	0.75	>0.99
	vehicle-injected POD3 $n = 3$ (f = 2,m = 1), POD28 $n = 3$ (f = 1,m = 2)	0.31	0.95	0.69	0.23	0.36	0.11
Lateral wall	AAV2.7m8-CAG-eGFP-injected POD3 $n = 3$ (f = 2,m = 1), POD28 $n = 3$ (f = 2,m = 1)	>0.99	>0.99	>0.99	0.77	0.34	0.18
	AAV2-CAG-eGFP-injected POD3 $n = 3$ (f = 2,m = 1), POD28 $n = 3$ (f = 2,m = 1)	>0.99	0.23	0.30	>0.99	0.09	0.14
	vehicle-injected POD3 $n = 3$ (f = 2,m = 1), POD28 $n = 3$ (f = 1,m = 2)	>0.99	0.12	0.25	>0.99	0.92	>0.99
Utricle	AAV2.7m8-CAG-eGFP-injected POD3 $n = 3$ (f = 2,m = 1), POD28 $n = 4$ (f = 2,m = 2)	0.32			0.55		
	AAV2-CAG-eGFP-injected POD3 $n = 4$ (f = 2,m = 2), POD28 $n = 4$ (f = 2,m = 2)	0.40			>0.99		
	vehicle-injected POD3 $n = 4$ (f = 2,m = 2), POD28 $n = 3$ (m = 3)	>0.99			>0.99		

f, female; m, male.
Kruskal-Wallis test with Dunn's multiple comparisons were used for statistical analyses. Comparisons were performed with non-surgery mice ($n = 3$: f = 1, m = 2).
[a]$p < 0.05$.

response to the viral capsid peptides (Figure 5A); only mouse 3 showed positive responses to VP1b and VP1c. Among the seven mice that were injected with AAV2-CAG-eGFP, six mice did not show an IFN-γ-positive response to the viral capsid peptides; only mouse 6 showed IFN-γ-positive responses to VP1b and VP1c (Figure 5B). We also performed the IFN-γ ELISpot assay on splenocytes from vehicle-injected mice and found that vehicle-injection did not trigger AAV capsid specific IFN-γ-secretion (Figures 5A and 5B). These results suggest that AAV-mediated inner ear gene delivery did not trigger significant IFN-γ-mediated antigen-specific T cell immune responses toward the AAV capsid.

AAV-mediated inner ear gene delivery causes an increase in selected cytokines and chemokines locally and systemically

Pro-inflammatory cytokines and chemokines play important roles in both innate and adaptive immunities. We examined the secretion of

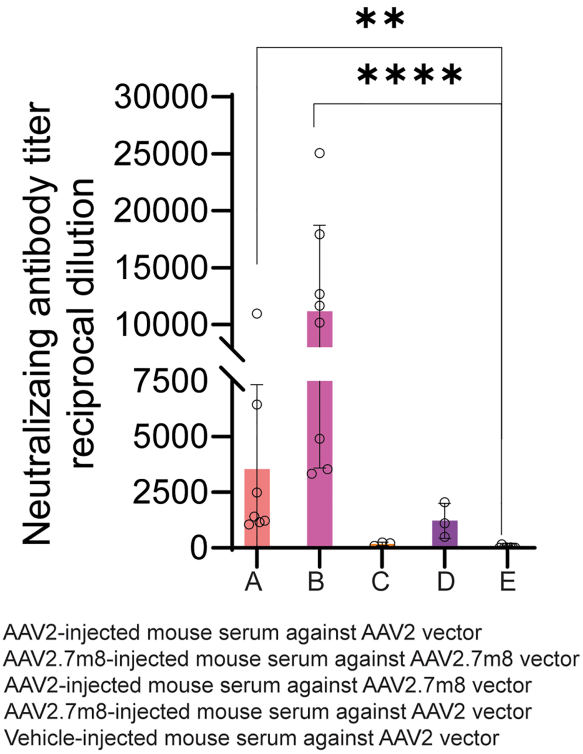

Figure 4. AAV-mediated inner ear gene delivery triggers neutralizing antibody production by POD28

The neutralizing antibody titers against AAV were quantified in mouse serum after AAV2-CAG-eGFP, AAV2.7m8-CAG-eGFP, or vehicle injections. The y axis shows viral neutralizing antibody titer by reciprocal dilution, and the x axis shows the identity of each group. Serum samples from AAV2-CAG-eGFP-injected mice against AAV2 (A, n = 7) showed statistically significant increase in neutralizing antibodies compared with serum samples from vehicle-injected mice (E, n = 8). Serum samples from AAV2.7m8-CAG-eGFP-injected mice against AAV2.7m8 (B, n = 8) also showed statistically significant increase in neutralizing antibodies compared with serum samples from vehicle-injected mice (E, n = 8). Serum samples from AAV2-CAG-eGFP-injected mice did not show significant increase in neutralizing antibodies against AAV2.7m8 (C, n = 3), and serum samples from AAV2.7m8-CAG-eGFP-injected mice did not show significant increase in neutralizing antibodies against AAV2 (D, n = 3). Kruskal-Wallis test with Dunn's multiple comparisons were used for statistical analysis. The error bars show standard deviations. $^{**}p < 0.01$, $^{****}p < 0.0001$.

pro-inflammatory cytokines and chemokines in the perilymph and serum of mice injected with AAV2.7m8-CAG-eGFP (1.0×10^{10} GC), AAV2-CAG-eGFP (1.0×10^{10} GC), or vehicle. Non-surgery mice were used as controls. The pro-inflammatory cytokines and chemokines that were assessed include IFN-γ, interleukin (IL)-1β, IL-2, IL-6, IL-10, tumor necrosis factor (TNF)-α, and CXCL1. The number of mice used in each experiment and their respective p values are summarized in Table S3. On POD3, increases in IL-6 and IL-1β were observed in perilymph samples from animals injected with AAV2.7m8-CAG-eGFP, AAV2-CAG-eGFP, and vehicle compared with non-surgery controls (Figure 6A) (IL-6, p = 0.022, p = 0.014, p = 0.0094; IL-1β, p = 0.033, p = 0.012, p = 0.044, respectively; Kruskal-Wallis test with Dunn's multiple comparisons). In addition, increases in TNF-α and IL-10 were also observed in perilymph samples from animals injected with AAV2-CAG-eGFP and vehicle compared with non-surgery controls (Figure 6A) (TNF-α, p = 0.012, p = 0.047; IL-10, p = 0.017, p = 0.039, respectively; Kruskal-Wallis test with Dunn's multiple comparisons). On POD28, most of the elevated pro-inflammatory cytokines and chemokines in perilymph normalized to levels similar to non-surgery animals (Figure 6C). However, TNF-α was elevated in mice injected with AAV2.7m8-CAG-eGFP compared with non-surgery mice (p = 0.036). On the other hand, serum samples from mice that were injected with AAV2.7m8-CAG-eGFP, AAV2-CAG-eGFP, or vehicle did not show any increase in pro-inflammatory cytokines/chemokines compared with non-surgery animals on POD3 and POD28 (Figures 6B and 6D). Overall, these results suggest that the elevation of pro-inflammatory cytokines and chemokines in perilymph is mostly transient, localized, and most likely induced by surgical trauma.

Viral genomes are not detected in the liver of injected mice on POD28

The liver is a key organ for metabolism. One common side effect seen in patients who received AAV-mediated gene therapy is drug-related hepatitis.[38] Since AAV-mediated inner ear gene delivery triggers the production of anti-AAV-neutralizing antibodies in the serum, we investigated whether localized AAV-mediated inner ear gene delivery caused systemic detection of AAV genomes in the liver of injected animals. Liver tissues were collected on POD3 and POD28 from animals that underwent inner ear injections with AAV2.7m8-CAG-eGFP (1.0×10^{10} GC), AAV2-CAG-eGFP (1.0×10^{10} GC), or vehicle. Extracted DNA samples from AAV2.7m8-CAG-eGFP-injected mice (POD3, n = 4, female = 2, male = 2; POD28, n = 6, female = 3, male = 3), AAV2-CAG-eGFP-injected mice (POD3, n = 4, female = 2, male = 3), POD28, n = 6, female = 3, male = 3), vehicle-injected mice (POD3, n = 4, female = 2, male = 2; POD28, n = 6, female = 2, male = 4), and age-matched non-surgery mice for control (n = 8, female = 4, male = 4) were analyzed by digital droplet PCR (ddPCR). The presence of viral genomes was assessed by probes targeting the eGFP sequence and compared with non-surgery mouse samples. On POD3, AAV2.7m8 genomes were detected in the liver of mice that underwent AAV2.7m8-CAG-eGFP injections. The AAV2 viral genomes were also detected in the liver of two out of three mice that underwent AAV2-CAG-eGFP injections, although the levels were lower than those seen in AAV2.7m8-CAG-eGFP-injected mice (Figure 7). Interestingly, by POD28, neither AAV2 nor AAV2.7m8 viral genomes were detected in the liver (Figure 7), even though the transgene (eGFP) delivered by these AAVs expressed abundantly in the cochlea (Figure S3C). This suggests that, although AAV genomes may be transiently detected in the liver of mice that underwent AAV-mediated inner ear gene delivery, these viral genomes were cleared by POD28.

DISCUSSION

The host immune response plays an important role in the success of AAV-mediated gene therapy.[39] It has been reported that host immune responses triggered by AAV can have a significant impact on the efficacy and safety of gene therapy.[9,40,41] The human inner

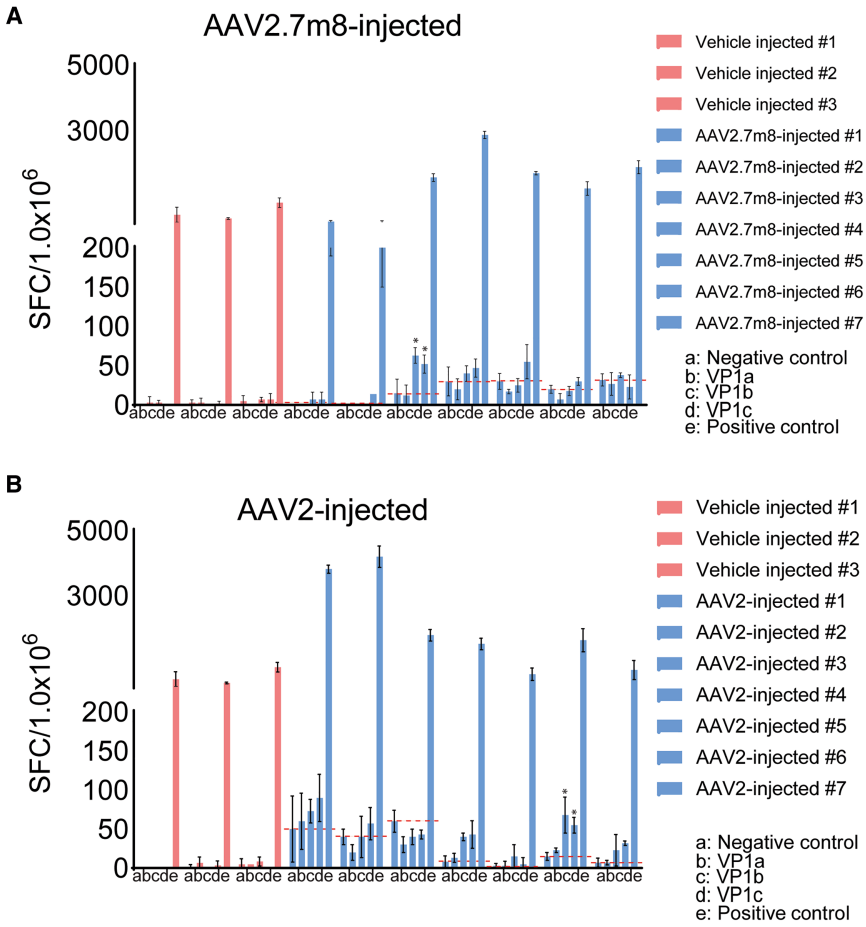

Figure 5. AAV-mediated inner ear gene delivery does not trigger a significant anti-capsid peripheral cellular immune response

Splenocytes (POD28) were stimulated *in vitro* with an overlapping peptide library spanning the VP1 sequence of AAV2.7m8 or AAV2 and analyzed using an IFN-γ ELISpot assay. Responses were considered positive when the number of spot-forming colonies (SFCs) per 1×10^6 cells were >50 and at least 3-fold higher than the negative control. The orange dashed lines show the value of negative controls. (A) The splenocytes from AAV2.7m8-CAG-eGFP-injected mice ($n = 7$) were tested and only mouse #3 showed an IFN-γ-positive response. (B) The splenocytes from AAV2-CAG-eGFP injected mice ($n = 7$) were tested and only mouse #6 showed an IFN-γ-positive response. The responses were considered positive when the number of SFCs per 1×10^6 cells were >50 and at least 3-fold higher than the negative control. Error bars represent standard devations.

ear was previously considered to be immune privileged due to its relatively isolated anatomical location. However, several studies have shown that the mammalian inner ear has an active immune system.[42] As the field of AAV-mediated inner ear gene therapy matures, it is important to examine in detail the host innate and adaptive immune responses triggered by AAV-mediated inner ear gene delivery.

Macrophages play a key role in the innate immune responses of the mammalian inner ear. We tracked the macrophages in *Cx3cr1*$^{GFP/GFP}$ mice after AAV-2.7m8-CAG-tdTomato injections at POD1, 3, 7, 14, 21 and 28. We observed that, starting at POD3, an increase in macrophages was detected near the spiral limbus, the osseous spiral lamina, and the basilar membrane. The number of macrophages peaked at POD14 and declined by POD28. We repeated the experiment with AAV2-CAG-tdTomato injection to *Cx3cr1*$^{GFP/GFP}$ mice and observed similar trends. Since *Cx3cr1*$^{GFP/GFP}$ mice may have altered immune responses due to the lack of CX3CR1, we repeated this experiment with C57BL/6 mice and quantified macrophages at POD3 and POD28. We found that, although the number of macrophages in sensory epithelium increased in mice after either AAV2.7m8-CAG-eGFP, AAV2-CAG-eGFP, or vehicle injections, only vehicle-injected mice showed a statistically significant increase in apical and middle turns of cochlea in the sensory epithelium on POD3, and the AAV2-CAG-eGFP-injected mice showed a statistically significant increase in the middle and basal turns in the lateral wall on POD3, when compared with non-surgery control mice. By POD28, the number of cochlear macrophages were similar between all injected and non-injected mice. In addition, we performed assays to assess the presence of pro-inflammatory cytokines and chemokines in the perilymph and serum samples from mice that underwent AAV-mediated inner ear gene delivery. Perilymph samples from AAV2.7m8-CAG-eGFP-injected mice, AAV2-CAG-eGFP-injected mice, and vehicle-injected mice on POD3 showed an increase in pro-inflammatory cytokines and chemokines such as IL-6 and IL-1β compared with non-surgery control mice. In addition, perilymph samples from AAV2-CAG-eGFP-injected mice and vehicle-injected mice on POD3 showed an increase TNF-α and IL-10 compared with non-surgery control mice. On the other hand, serum samples from all injected animals did not show a significant increase in cytokines compared with non-injected mice on both POD3 and POD28. Overall, these results suggest that the innate immune responses observed after AAV-mediated inner ear gene delivery are mainly caused by surgical trauma and not by AAV vectors themselves.

Regarding the adaptive immune responses, the production of anti-AAV neutralizing antibodies plays an important role in the host immune responses for AAV-mediated gene therapies. In fact, for some AAV-mediated gene therapy clinical trials, the presence of pre-existing anti-AAV neutralizing antibodies is an exclusion criterion for trial enrollment.[12,43] Anti-AAV neutralizing antibodies could significantly interfere with AAV-mediated gene delivery.[9] However, some

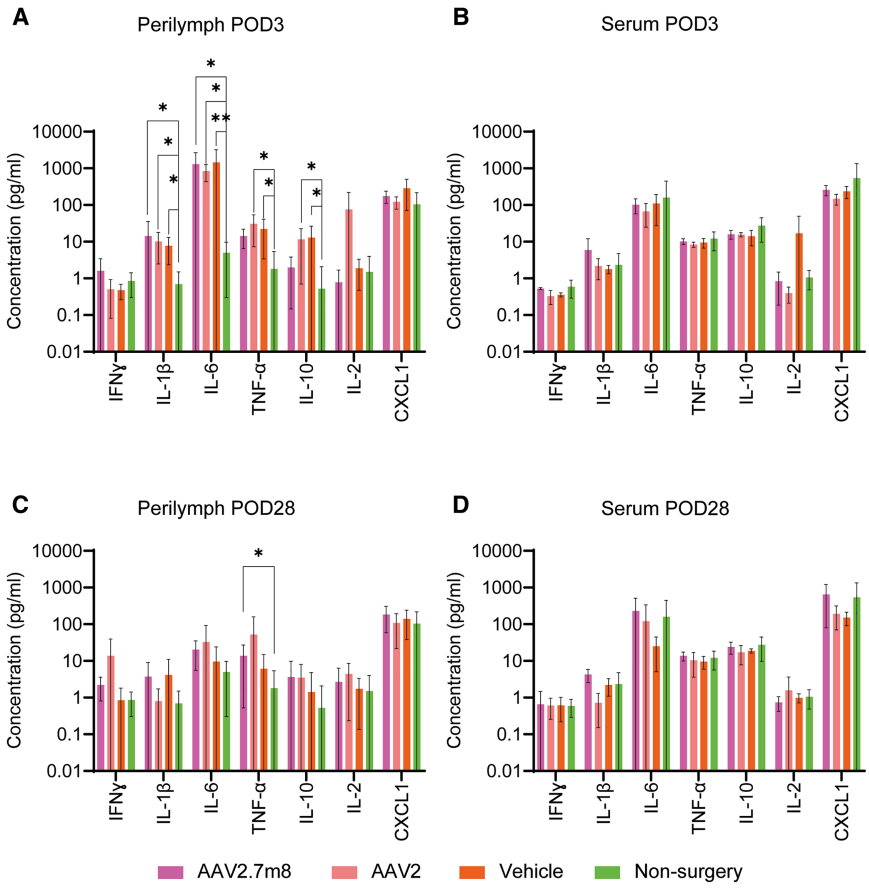

Figure 6. Assessment of pro-inflammatory cytokine and chemokine activation in response to AAV-mediated inner ear gene delivery

The levels of pro-inflammatory cytokines and chemokines are assessed in perilymph and serum samples from AAV2.7m8-CAG-eGFP-injected mice (POD3 perilymph $n = 4$ [female = 2 and male = 2], POD3 serum $n = 3$ [female = 2 and male = 1], POD28 perilymph and serum $n = 6$ [female = 3 and male = 3]), AAV2-CAG-eGFP-injected mice (POD3 perilymph $n = 4$ [female = 2 and male = 2], POD3 serum $n = 4$ [female = 2 and male = 2], POD28 perilymph $n = 5$ [female = 3 and male = 2], POD28 serum $n = 6$ [female = 3 and male = 3]), and vehicle-injected mice (POD3 perilymph and serum $n = 4$ [female = 2 and male = 2], POD28 perilymph and serum $n = 6$ [female = 2 and male = 4]) were evaluated. Perilymph and serum samples from non-surgery mice ($n = 9$ [female = 4 and male = 5]) were used as controls. (A) Perilymph of all injected groups at POD3 demonstrated increases in IL-1β and IL-6 compared with the non-surgery group. AAV2-CAG-eGFP and vehicle-injected groups also showed increases in TFN-α and IL-10 compared with the non-surgery group. (B) Serum at POD3 from injected groups did not show significant differences in cytokine/chemokine levels compared with non-surgery samples. (C) Perilymph samples at POD28 from AAV2.7m8-CAG-eGFP-injected group showed an increase in TFN-α compared with non-surgery controls. (D) Serum at POD28 from injected groups do not show significant differences in cytokine/chemokine levels compared with non-surgery samples. Kruskal-Wallis test with Dunne's multiple comparisons were used for statistical analysis. Error bars show standard deviations. $^{*}p < 0.05$, $^{**}p < 0.01$.

studies have shown that the presence of anti-AAV neutralizing antibodies in the serum may not interfere with AAV-mediated gene therapy if the viral vector is administrated locally, such as in the subretinal space of the eye.[44–46] Another study showed that direct injection of AAVs into the brain of patients with neurodegenerative diseases who have pre-existing anti-AAV neutralizing antibodies did not cause severe adverse effects and showed similar treatment efficacy compared with patients who did not have pre-existing neutralizing antibodies against AAV.[44] Our results showed that local injections of AAV2.7m8-CAG-eGFP or AAV2-CAG-eGFP into the mouse inner ear led to the production of neutralizing antibodies against these viral vectors by POD28 in the serum. After AAV injection into the perilymph, the pathways through which the viral vectors can reach the target cells in the inner ear are not completely understood. However, unlike AAV-mediated gene delivery into the retina, which rarely results in the production of neutralizing antibodies,[47] AAV-mediated inner ear gene delivery does trigger production of neutralizing antibodies. An important question that still needs to be addressed is whether pre-existing neutralizing antibodies against naturally occurring AAVs could affect subsequent AAV-mediated inner ear gene delivery. A study showed intravenous injection of AAV-PHP.B caused neutralizing antibodies in serum, but this did not affect the viral transduction of subsequent AAV-mediated gene delivery to the cerebellum.[48] However, a seroprevalence study showed a high prevalence of pre-existing neutralizing antibodies against AAVs globally, which could affect even the initial dose of AAV-mediated gene therapy due to cross-reactivities.[49,50] In this study, we also examined the *in vitro* cross-reactivity between AAV2 and AAV2.7m8 by using the serum samples from mice injected with either of these viral vectors. AAV2.7m8 is a synthetic AAV that was modified from AAV2 by adding 10 additional amino acids to its viral capsid sequence.[51] Therefore, we expected cross-reactivity between these two serotypes. To our surprise, the cross-reactivity was very limited. Currently, there are several ongoing inner ear gene therapy clinical trials targeting the non-syndromic autosomal recessive hereditary hearing loss DFNB9, and no significant adverse effects related to neutralizing antibodies have been reported.[7,8] Additional studies are needed to examine the cross-reactivities of various AAV serotypes for inner ear gene delivery.

ELISpot assays were performed to evaluate whether AAV-mediated inner ear gene delivery induced antigen-specific IFN-γ secretion by cytotoxic T cells in the spleen. Both AAV2-CAG-eGFP and AAV2.7m8-CAG-eGFP-injected mice showed minimal

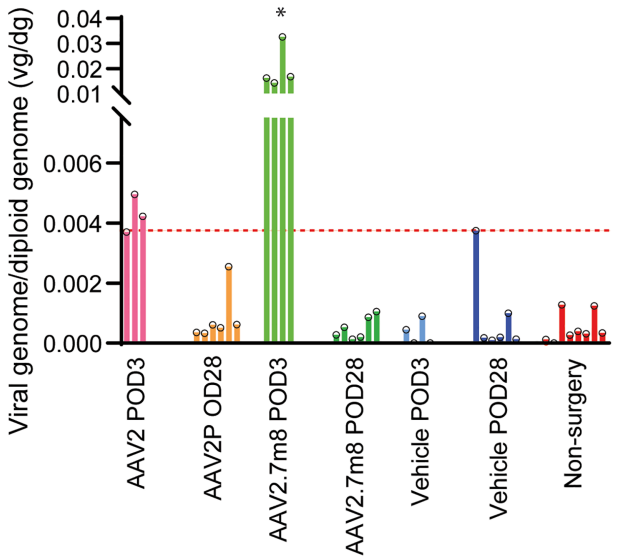

Figure 7. Vector biodistribution in the liver after AAV-mediated inner ear gene delivery

Extracted DNA from liver of AAV2.7m8-CAG-eGFP-injected mice (POD3, *n* = 4; POD28, *n* = 6), AAV2-CAG-eGFP-injected mice (POD3, *n* = 4; POD28, *n* = 6), vehicle-injected mice (POD3, *n* = 4; POD28: *n* = 6), and non-surgery mice (*n* = 8) were amplified by ddPCR, and viral genomes were detected using probes targeting the eGFP sequence. Albumin was used as a reference. At POD3, viral genomes were detected in the liver samples from all AAV2.7m8-CAG-eGFP-injected mice and two out of three AAV2-CAG-eGFP-injected mice. At POD28, viral genome detection levels in all injected mice returned to the level of non-surgery mice. The orange dashed line shows the positivity threshold from background defined from non-surgery mice. * indicates values above baseline in all samples.

IFN-γ secretion against capsid peptide of respective AAV vectors. Only one out of seven mice in each group showed positivity. The cellular component of the adaptive immune response may have significant impact on the long-term outcomes of AAV-mediated gene therapy.[9,52] Our results showed that a one-time local injection of AAVs into the inner ear did not induce systemic cytotoxic T cell responses. To examine the systemic impact of AAV-mediated inner ear gene delivery, we evaluated whether viral genomes are detected in the liver. Our results showed that, on POD3, viral genomes were detected in the liver tissues of both AAV2-CAG-eGFP- and AAV2.7m8-CAG-eGFP-injected mice. The AAV vectors injected into the inner ear might travel from the inner ear to other organ systems through the cochlear aqueduct and/or through blood vessels supplying the inner ear.[1,53] However, by POD28, viral genomes in the hepatocytes were barely detectable.[54]

In this study, we investigated the innate and adaptive immune responses triggered by a single injection of AAV2 or AAV2.7m8 into the adult mouse inner ear. Our results indicate that the innate immune responses were mainly triggered locally by the surgical trauma. For the humoral component of adaptive immune responses, anti-AAV neutralizing antibodies were detected in the serum of injected animals. For the cellular component of adaptive immune responses, secretion of AAV-capsid specific IFN-γ by cytotoxic T cells was detected in only one out of seven mice, and the reaction is considered mild compared with positive controls. Our results indicate that the host innate and adaptive immune responses triggered by AAV-mediated inner ear gene delivery are limited and mild, which suggests that the host immune system is less likely to interfere with the efficacy and safety of inner ear gene therapy.

MATERIALS AND METHODS

Animal surgery

Animal surgery was approved by the Animal Care and Use Committee at the National Institute on Deafness and Other Communication Disorders (NIDCD ASP1378). All animal procedures were done in compliance with the ethical guidelines and regulations set forth by the Animal Care and Use Committee at NIDCD. Adult (8- to 10-week-old) C57BL/6 and B6.129P2(Cg)-*Cx3cr1*^{tm1Litt}/J (described as *Cx3cr1*$^{GFP/GFP}$ in the manuscript) mice were used for this project. Inner ear gene delivery was performed via the PSCC approach as previously described.[18] Briefly, anesthesia was induced using isoflurane gas (Baxter, cat# 1001936040, Deerfield, IL, USA) through a nose cone for the mouse at a flow rate of 0.5 L/min. A post-auricular incision was made with scissors. The subcutaneous tissues were bluntly dissected to expose the PSCC. The facial nerve was identified after dividing the sternocleidomastoid muscle. To locate the PSCC, the facial nerve was followed superiorly and posteriorly. The PSCC was localized approximately 3–4 mm posteriorly from the ear canal. To expose lumen of the ossified PSCC, a 27G hypodermic needle was used to enter the canal lumen. A Nanoliter Microinjection System (World Precision Instruments, Nanoliter2000, Sarasota, FL, USA) was used in conjunction with a polyethylene tube (MicroLumen, 0.1222 mm diameter, Oldsmar, FL, USA) attached to a glass micropipette (Shutter Instruments, 1.0 mm outer diameter, 0.75 mm inner diameter, Novato, CA, USA) to load the viral vector. The polyethylene tube was inserted into the PSCC lumen. GLUture topical tissue adhesive (World Precision Instruments, cat# 503763, Sarasota, FL, USA) was used to secure the injection tubing around the PSCC fenestration to prevent perilymph leakage from the injection site. Approximately 1 μL of virus of AAV2-CAG-eGFP (1.0×10^{13} GC/mL) and AAV2.7m8-CAG-eGFP (1.0×10^{13} GC/mL) and AAV2-CAG-tdTomato (1.0×10^{13} GC/mL) and AAV2.7m8-CAG-tdTomato (1.1×10^{13} GC/mL) were injected into the PSCC of each animal. Injections were performed only in the left ear of each animal. The posterior semicircular canalostomy was sealed with a small piece of muscle with GLUture topical tissue adhesive and the incision was closed with 5-0 Vicryl sutures (Ethicon, cat# J303H, Raritan, NJ, USA) and GLUture topical tissue adhesive. All injected animals were injected in the left ear only. Age-matched non-injected mice were used as non-injected controls.

Immunohistochemistry and quantifications

Mice were euthanized by CO_2 asphyxiation followed by decapitation. Temporal bones were harvested and fixed with 4% paraformaldehyde diluted in PBS, followed by decalcification in 120 mM EDTA

(Thermo Fisher Science Invitrogen, cat# AM9261, Waltham, MA, USA), for 3–5 days. The cochlear tissues were micro-dissected into base, middle, and apical turns. The length of each turn (mean ± SD) was 1.67 ± 0.14 mm for the apical turn, 1.44 ± 0.13 mm for the middle turn, and 2.07 ± 0.21 for the basal turn. The approximate frequency range is 5–12 kHz for the apical turn, 12–24 kHz for the middle turn, and 24–64 kHz for the basal turn.[55] Tissues were washed in PBS and blocked/permeabilized with 2% BSA and goat serum with 0.5% Triton X-100 in PBS for 2 h. Incubation with primary antibody was performed overnight at 4°C. Antibodies against the T cell maker CD3 (1:200, BD Bioscience, cat# BDB562163, Franklin Lakes, NJ, USA) and against the macrophage marker IBA1 (1:200, Invitrogen, cat# PA5-27436, Carlsbad, CA, USA) were used to quantify the presence of T cells and macrophages in the inner ear tissues, respectively. The antibody against CD3 markers was tested in the thymus, spleen, and bone marrow specimens to confirm its ability to detect T cells before its use in the cochlea (data not shown). For the secondary antibodies, Alexa Fluor 546 goat anti-rabbit immunoglobulin (Ig) G (1:500, Thermo Fisher Science Invitrogen, cat# A-11035), and Alexa Fluor 647 goat anti-rat IgG (1:500, Thermo Fisher Science Invitrogen, cat# A-21247) were applied for 2 h at room temperature. Phalloidin-Atto 390, was used to label F-actin (1:50, Sigma-Aldrich, cat#50556, St. Louis, MO, USA). Hoechst stain was used for label nuclei (1:300, Life Technologies, cat# 62,249, Carlsbad, CA, USA). Primary and secondary antibodies were diluted in 1× PBS. For cross-sections, cochleae were collected and fixed overnight with 4% paraformaldehyde diluted in PBS (Electron Microscopy science, cat#15710, Hatfield, PA, USA), followed by decalcification in EDTA for 3–5 days and embedded in SCEM freezing media (Section-Lab, cat# C-EM001, Kanagawa, Japan); 10-μm sections were collected using Leica CM3050S cryostat. Images were obtained using z stack with Zeiss LSM900 confocal microscope (Zeiss Microimaging, Jena, Germany) with Plan-Neofluaromat ×40/1.3 Oil DIC M27, Plan-Neofluar ×20/0.80 NA, Plan-Apochromat 63×/1.4NA objectives. Macrophages were identified using anti-IBA1 antibody, and T cell were identified with anti-CD3 antibody in z stack images of whole mount with 40× magnifications and manually counted, and the average from two location in each cochlear region (base, middle turn, and apex) of the specimen was taken. Whole-mount images of the cochlea from *Cx3cr1*$^{GFP/GFP}$ mice were processed with PFA and EDTA as mentioned above, and dissected into basal, middle, and apical turns to evaluate changes in macrophage number on POD 1, 3, 7, 14, 21, 28; animals that did not undergo surgery were used as controls (non-surgery control). Antibody against GFP (1:1000, Abcam, cat# ab13970, Boston, MA, USA) was used to label eGFP, and anti-CD68 antibody (1:200, Bio-Rad, cat# MCA1957) was used to label macrophages. Alexa Fluor 647 goat anti-rat IgG (1:500, ThermoFisher Science Invitrogen, cat# A-21247, Waltham, MA) and Alexa Fluor 488 goat anti-chicken IgG (1:500, Thermo Fisher Science Invitrogen, cat# A-11039) were used as secondary antibodies. Phalloidin-Atto 390 was used to label F-actin (1:50, Sigma-Aldrich, cat# 50556) and Hoechst stain was used for label nuclei. z stack images were captured with a Plan-Neofluaromat 40x/1.3 Oil DIC M27 objective. Three-dimensional view of confocal images was processed with Imaris Viewer 10.1.1 (Oxford Instruments, Abington, UK).

The quantification of cochlear hair cells transduction was performed as follows. The total number of inner and outer hair cells was counted, and the number of eGFP-expressing inner and outer hair cells was assessed from two separate images in each cochlear turn (apex, middle, and basal turns). The transduction rates of each cochlear turn for AAV2.7m8-CAG-eGFP and AAV2-CAG-eGFP are summarized in Table S1.

Perilymph collection

Perilymph was collected through the PSCC approach on POD3 and POD 28 as previously described.[56] A small drop of Vetbond Tissue Adhesive (3M, cat# 1469SB, St. Paul, MN, USA) was applied to the surface of the PSCC. A small fenestration was made on the surface of PSCC through the hardened tissue glue. The first 1.1 μL of perilymph was collected using a micro-pipette.[56,57] Collected perilymph was frozen immediately and kept at −80 C° until processing.

Viral neutralizing antibody titer assay

Serum samples were collected from animals that were injected with either AAV2-CAG-eGFP, AAV2.7m8-CAG-eGFP, or vehicle on POD28. COS-7 cells (ATCC, cat# CRL-1651, Gaithersburg, MD, USA) were cultured in DMEM at 7,000 cells/well and incubated for 24 h in a 96-well plate. Serum was serially diluted, and the diluted serum was applied to COS-7 cells along with 2.5×10^9 GC of AAV2-CAG-eGFP or AAV2.7m8-CAG-eGFP vectors for 1 hour. For the positive control, the COS-7 cells were incubated with viral vector with fetal bovine serum (FBS) (Neuromics, cat# FBS001, Edina, MN, USA). For the negative control, we incubated COS-7 cells with culture media without FBS. After 48 h of incubation, cells were treated with trypsin and analyzed for GFP expression using Sony SA3800 spectral cell analyzer (Sony Biotechnology, San Jose, CA, USA) to assess the presence of neutralizing antibodies against AAVs. For each serum dilution, the experiment was performed in triplicates. The average GFP expression (%) was calculated and normalized with positive and negative controls which were performed simultaneously for each assay, and plotted to a nonlinear regression curve. 50% of GFP expression of the positive control was calculated to obtain neutralizing antibody titer.

IFN-γ ELISpot assay

Splenocytes were isolated from animals four weeks after surgery, and IFN-γ ELISpot assay was performed according to manufacturer's instructions (MABTech, ELISpot Mouse IFN-γ, Nacka Strand, Sweden). Briefly, splenocytes were stimulated *in vitro* for 48 h with overlapping peptides spanning the AAV VP1 capsid sequence and divided into three pools (VP1a, VP1b, VP1c, and 15-mers overlapping by 10 aa). Unstimulated cells with media only were used as negative controls, and cells that were stimulated with Concanavalin A were used as positive controls for cytokine secretion. Spot-forming colonies were determined using the ELISpot reader ELR07

(Autoimmun Diagnostika (AID) GMBH, Strassberg, Germany) and analyzed with AID ELISpot Reader Software V7.0.

Pro-inflammatory cytokine and chemokine measurement

Seven pro-inflammatory cytokines and chemokines, IFN-γ, IL-1β, IL-2, IL-6, CXCL1, IL-10 and TNF-α, were measured in perilymph and serum samples using electrochemiluminescence V-PLEX proinflammatory panel 1 mouse kit (Meso Scale Diagnostics LLC, cat# K15048D, Rockville, MD, USA). Serum samples from mice were diluted 2-fold and perilymph samples were diluted 25-fold, and a total 25 μL of samples were applied to 96-well plate per the manufacturer's instructions. The standard calibrators of each cytokine and chemokine were assessed in the same plate to generate a standard curve. The results from each sample were extrapolated into concentrations from the standard curve. The samples below the detection range of each cytokine and chemokine were not included in data analysis. Computations were conducted using MSD Discovery Workbench 4.0 Workbench (Meso Scale Diagnostics).[58]

ddPCR genome titer assay

DNA samples were extracted from the liver of mice that underwent either AAV2.7m8, AAV2, or vehicle injection on POD3 and POD28. DNA from livers of non-surgery mice were used as a negative control. Droplet digital PCR was performed to detect the viral genome in the liver tissue by using the ddPCR system QX200 (Bio-Rad). The probe and primers for AAVs were designed to target the eGFP sequence (GenBank: U57608) and the albumin reference gene [*Alb* gene, NM_009654]. The sequences of the primers are: forward eGFP primer 5′ AGTCCGCCCTGAGCAAAGA 3′, reverse eGFP primer 5′ GCGGTCACGAACTCCAGC 3′. the sequence for eGFP probe is 5′ CAACGAGAAGCGCGATCACATGGTC 3′. For the reference gene, we used mouse albumin (*Alb*) ddPCR Copy Number Determination Assay (Bio-Rad, cat # 10042961). The PCR reactions were performed according to the manufacturer's protocol with ddPCR Supermix for probe and duplicated for each sample. The PCR protocol is as follows: 95°C for 10 min, followed by 40 cycles of 94°C for 30 s and 60°C for 1 min, and a final 98°C heat treatment for 10 min. The PCR plate was subsequently scanned on a QX200 Droplet Digital PCR System (Bio-Rad) and the data were analyzed with QuantaSoft software (Bio-Rad).

Statistics

GraphPad Prism version 10.1 (GraphPad, Boston, MA) was used for statistical analysis. We performed normality test on our data to assess whether they followed a normal distribution. When the data did not follow a normal distribution, non-parametric tests were used for the analyses. The statistical test used in each experiment was described in the results section. A p value of less than 0.05 indicates statistical significance.

DATA AVAILABILITY

All data are contained in the article and supplemental information. Unique reagents are available from the communicating authors following completion of a simple National Institutes of Health Material Transfer Agreement.

ACKNOWLEDGMENTS

This research was supported (in part) by the Intramural Research Program of the NIH, NIDCD, DC000082-02 to W.W.C., and DC000039 to T.B.F. We thank Dr. Cathy Yea Won Sung and Dr. Lisa L. Cunningham from NIDCD for assistance with cytokine evaluation and critical comments. We thank Dr. Giovanni Di Pasquale and Dr. John A. Chiorini from NIDCR and the Flow Cytometry Core Facility at NCI for their assistance with the neutralizing antibody assay, and Ms. Manon Loirat for assistance with ELISpot assay. We thank Dr. Elizabeth C. Driver from NIDCD for assistance with imaging. We thank Dr. Clint Allen for critical comments. We are grateful for the NIDCD animal facility staff for caring for our mice.

AUTHOR CONTRIBUTIONS

Y.I., W.W.C., G.G., and O.A. conceived and designed the study. Y.I., J.Z., G.G., and Y.Y. performed the experiment. Y.I., J.Z., G.G., Y.Y., W.W.C., C.L., and O.A. analyzed the data. W.W.C., C.L., O.A., M.G., K.I., T.B.F., M.H., and R.O. supervised the work. Y.I. and W.W.C. wrote the manuscript with the participation of all authors.

DECLARATION OF INTERESTS

The authors declare that they have no conflict of interest with the contents of the article.

SUPPLEMENTAL INFORMATION

Supplemental information can be found online at https://doi.org/10.1016/j.omtm.2025.101456.

REFERENCES

1. Salt, A.N., and Hirose, K. (2018). Communication pathways to and from the inner ear and their contributions to drug delivery. Hear. Res. *362*, 25–37. https://doi.org/10.1016/j.heares.2017.12.010.

2. Naso, M.F., Tomkowicz, B., Perry, W.L., 3rd, and Strohl, W.R. (2017). Adeno-Associated Virus (AAV) as a Vector for Gene Therapy. BioDrugs *31*, 317–334. https://doi.org/10.1007/s40259-017-0234-5.

3. Chien, W.W., Monzack, E.L., McDougald, D.S., and Cunningham, L.L. (2015). Gene therapy for sensorineural hearing loss. Ear Hear. *36*, 1–7. https://doi.org/10.1097/AUD.0000000000000088.

4. Balakrishnan, B., and Jayandharan, G.R. (2014). Basic biology of adeno-associated virus (AAV) vectors used in gene therapy. Curr. Gene Ther. *14*, 86–100. https://doi.org/10.2174/1566523214666140302193709.

5. Askew, C., and Chien, W.W. (2020). Adeno-associated virus gene replacement for recessive inner ear dysfunction: Progress and challenges. Hear. Res. *394*, 107947. https://doi.org/10.1016/j.heares.2020.107947.

6. Zhang, Z., Wang, J., Li, C., Xue, W., Xing, Y., and Liu, F. (2020). Gene therapy development in hearing research in China. Gene Ther. *27*, 349–359. https://doi.org/10.1038/s41434-020-0177-1.

7. Qi, J., Tan, F., Zhang, L., Lu, L., Zhang, S., Zhai, Y., Lu, Y., Qian, X., Dong, W., Zhou, Y., et al. (2024). AAV-Mediated Gene Therapy Restores Hearing in Patients with DFNB9 Deafness. Adv. Sci. *11*, e2306788. https://doi.org/10.1002/advs.202306788.

8. Lv, J., Wang, H., Cheng, X., Chen, Y., Wang, D., Zhang, L., Cao, Q., Tang, H., Hu, S., Gao, K., et al. (2024). AAV1-hOTOF gene therapy for autosomal recessive deafness 9: a single-arm trial. Lancet *403*, 2317–2325. https://doi.org/10.1016/S0140-6736(23)02874-X.

9. Manno, C.S., Pierce, G.F., Arruda, V.R., Glader, B., Ragni, M., Rasko, J.J., Ozelo, M.C., Hoots, K., Blatt, P., Konkle, B., et al. (2006). Successful transduction of liver in hemophilia by AAV-Factor IX and limitations imposed by the host immune response. Nat. Med. *12*, 342–347. https://doi.org/10.1038/nm1358.

10. Amado, D., Mingozzi, F., Hui, D., Bennicelli, J.L., Wei, Z., Chen, Y., Bote, E., Grant, R.L., Golden, J.A., Narfstrom, K., et al. (2010). Safety and efficacy of subretinal readministration of a viral vector in large animals to treat congenital blindness. Sci. Transl. Med. *2*, 21ra16. https://doi.org/10.1126/scitranslmed.3000659.2/21/21ra16.

11. Mingozzi, F., and Büning, H. (2015). Adeno-Associated Viral Vectors at the Frontier between Tolerance and Immunity. Front. Immunol. *6*, 120. https://doi.org/10.3389/fimmu.2015.00120.

12. Mingozzi, F., and High, K.A. (2013). Immune responses to AAV vectors: overcoming barriers to successful gene therapy. Blood *122*, 23–36. https://doi.org/10.1182/blood-2013-01-306647.

13. Duan, D. (2018). Systemic AAV Micro-dystrophin Gene Therapy for Duchenne Muscular Dystrophy. Mol. Ther. *26*, 2337–2356. https://doi.org/10.1016/j.ymthe.2018.07.011.

14. Wilson, J.M., and Flotte, T.R. (2020). Moving Forward After Two Deaths in a Gene Therapy Trial of Myotubular Myopathy. Hum. Gene Ther. *31*, 695–696. https://doi.org/10.1089/hum.2020.182.

15. Parham, P. (2021). The Immune System, Fifth edition (W.W. Norton & Company).

16. Dunkelberger, J.R., and Song, W.C. (2010). Complement and its role in innate and adaptive immune responses. Cell Res. *20*, 34–50. https://doi.org/10.1038/cr.2009.139.

17. Guo, R.F., and Ward, P.A. (2005). Role of C5a in inflammatory responses. Annu. Rev. Immunol. *23*, 821–852. https://doi.org/10.1146/annurev.immunol.23.021704.115835.

18. Zhu, J., Choi, J.W., Ishibashi, Y., Isgrig, K., Grati, M., Bennett, J., and Chien, W. (2021). Refining surgical techniques for efficient posterior semicircular canal gene delivery in the adult mammalian inner ear with minimal hearing loss. Sci. Rep. *11*, 18856. https://doi.org/10.1038/s41598-021-98412-y.

19. Jung, S., Aliberti, J., Graemmel, P., Sunshine, M.J., Kreutzberg, G.W., Sher, A., and Littman, D.R. (2000). Analysis of fractalkine receptor CX(3)CR1 function by targeted deletion and green fluorescent protein reporter gene insertion. Mol. Cell Biol. *20*, 4106–4114. https://doi.org/10.1128/mcb.20.11.4106-4114.2000.

20. Hirose, K., Discolo, C.M., Keasler, J.R., and Ransohoff, R. (2005). Mononuclear phagocytes migrate into the murine cochlea after acoustic trauma. J. Comp. Neurol. *489*, 180–194. https://doi.org/10.1002/cne.20619.

21. Sautter, N.B., Shick, E.H., Ransohoff, R.M., Charo, I.F., and Hirose, K. (2006). CC chemokine receptor 2 is protective against noise-induced hair cell death: studies in CX3CR1(+/GFP) mice. J. Assoc. Res. Otolaryngol. *7*, 361–372. https://doi.org/10.1007/s10162-006-0051-x.

22. Sato, E., Shick, H.E., Ransohoff, R.M., and Hirose, K. (2008). Repopulation of cochlear macrophages in murine hematopoietic progenitor cell chimeras: the role of CX3CR1. J. Comp. Neurol. *506*, 930–942. https://doi.org/10.1002/cne.21583.

23. Sato, E., Shick, H.E., Ransohoff, R.M., and Hirose, K. (2010). Expression of fractalkine receptor CX3CR1 on cochlear macrophages influences survival of hair cells following ototoxic injury. J. Assoc. Res. Otolaryngol. *11*, 223–234. https://doi.org/10.1007/s10162-009-0198-3.

24. Hirose, K., Li, S.Z., Ohlemiller, K.K., and Ransohoff, R.M. (2014). Systemic lipopolysaccharide induces cochlear inflammation and exacerbates the synergistic ototoxicity of kanamycin and furosemide. J. Assoc. Res. Otolaryngol. *15*, 555–570. https://doi.org/10.1007/s10162-014-0458-8.

25. Kaur, T., Zamani, D., Tong, L., Rubel, E.W., Ohlemiller, K.K., Hirose, K., and Warchol, M.E. (2015). Fractalkine Signaling Regulates Macrophage Recruitment into the Cochlea and Promotes the Survival of Spiral Ganglion Neurons after Selective Hair Cell Lesion. J. Neurosci. *35*, 15050–15061. https://doi.org/10.1523/JNEUROSCI.2325-15.2015.

26. Kaur, T., Hirose, K., Rubel, E.W., and Warchol, M.E. (2015). Macrophage recruitment and epithelial repair following hair cell injury in the mouse utricle. Front. Cell. Neurosci. *9*, 150. https://doi.org/10.3389/fncel.2015.00150.

27. Hirose, K., Rutherford, M.A., and Warchol, M.E. (2017). Two cell populations participate in clearance of damaged hair cells from the sensory epithelia of the inner ear. Hear. Res. *352*, 70–81. https://doi.org/10.1016/j.heares.2017.04.006.

28. Kaur, T., Clayman, A.C., Nash, A.J., Schrader, A.D., Warchol, M.E., and Ohlemiller, K.K. (2019). Lack of Fractalkine Receptor on Macrophages Impairs Spontaneous Recovery of Ribbon Synapses After Moderate Noise Trauma in C57BL/6 Mice. Front. Neurosci. *13*, 620. https://doi.org/10.3389/fnins.2019.00620.

29. Liu, W., Danckwardt-Lilliestöm, N., Schrott-Fischer, A., Glueckert, R., and Rask-Andersen, H. (2021). Distribution of Immune Cells Including Macrophages in the Human Cochlea. Front. Neurol. *12*, 781702. https://doi.org/10.3389/fneur.2021.781702.

30. Okano, T., Nakagawa, T., Kita, T., Kada, S., Yoshimoto, M., Nakahata, T., and Ito, J. (2008). Bone marrow-derived cells expressing Iba1 are constitutively present as resident tissue macrophages in the mouse cochlea. J. Neurosci. Res. *86*, 1758–1767. https://doi.org/10.1002/jnr.21625.

31. Holness, C.L., and Simmons, D.L. (1993). Molecular cloning of CD68, a human macrophage marker related to lysosomal glycoproteins. Blood *81*, 1607–1613.

32. Chavan, S.S., Pavlov, V.A., and Tracey, K.J. (2017). Mechanisms and Therapeutic Relevance of Neuro-immune Communication. Immunity *46*, 927–942. https://doi.org/10.1016/j.immuni.2017.06.008.

33. Noda, M., Doi, Y., Liang, J., Kawanokuchi, J., Sonobe, Y., Takeuchi, H., Mizuno, T., and Suzumura, A. (2011). Fractalkine attenuates excito-neurotoxicity via microglial clearance of damaged neurons and antioxidant enzyme heme oxygenase-1 expression. J. Biol. Chem. *286*, 2308–2319. https://doi.org/10.1074/jbc.M110.169839.

34. Stothert, A.R., and Kaur, T. (2021). Innate Immunity to Spiral Ganglion Neuron Loss: A Neuroprotective Role of Fractalkine Signaling in Injured Cochlea. Front. Cell. Neurosci. *15*, 694292. https://doi.org/10.3389/fncel.2021.694292.

35. Cardona, S.M., Mendiola, A.S., Yang, Y.C., Adkins, S.L., Torres, V., and Cardona, A.E. (2015). Disruption of Fractalkine Signaling Leads to Microglial Activation and Neuronal Damage in the Diabetic Retina. ASN Neuro *7*, 1759091415608204. https://doi.org/10.1177/1759091415608204.

36. Mendiola, A.S., Garza, R., Cardona, S.M., Mythen, S.A., Lira, S.A., Akassoglou, K., and Cardona, A.E. (2016). Fractalkine Signaling Attenuates Perivascular Clustering of Microglia and Fibrinogen Leakage during Systemic Inflammation in Mouse Models of Diabetic Retinopathy. Front. Cell. Neurosci. *10*, 303. https://doi.org/10.3389/fncel.2016.00303.

37. Wu, Z., Asokan, A., and Samulski, R.J. (2006). Adeno-associated virus serotypes: vector toolkit for human gene therapy. Mol. Ther. *14*, 316–327. https://doi.org/10.1016/j.ymthe.2006.05.009.

38. Mucke, M.M., Fong, S., Foster, G.R., Lillicrap, D., Miesbach, W., and Zeuzem, S. (2024). Adeno-associated viruses for gene therapy - clinical implications and liver-related complications, a guide for hepatologists. J. Hepatol. *80*, 352–361. https://doi.org/10.1016/j.jhep.2023.10.029.

39. Vandamme, C., Adjali, O., and Mingozzi, F. (2017). Unraveling the Complex Story of Immune Responses to AAV Vectors Trial After Trial. Hum. Gene Ther. *28*, 1061–1074. https://doi.org/10.1089/hum.2017.150.

40. Mingozzi, F., Maus, M.V., Hui, D.J., Sabatino, D.E., Murphy, S.L., Rasko, J.E.J., Ragni, M.V., Manno, C.S., Sommer, J., Jiang, H., et al. (2007). CD8(+) T-cell responses to adeno-associated virus capsid in humans. Nat. Med. *13*, 419–422. https://doi.org/10.1038/nm1549.

41. Muhuri, M., Maeda, Y., Ma, H., Ram, S., Fitzgerald, K.A., Tai, P.W., and Gao, G. (2021). Overcoming innate immune barriers that impede AAV gene therapy vectors. J. Clin. Investig. *131*, e143780. https://doi.org/10.1172/JCI143780.

42. Ishibashi, Y., Sung, C.Y.W., Grati, M., and Chien, W. (2023). Immune responses in the mammalian inner ear and their implications for AAV-mediated inner ear gene therapy. Hear. Res. *432*, 108735. https://doi.org/10.1016/j.heares.2023.108735.

43. Mingozzi, F., and High, K.A. (2017). Overcoming the Host Immune Response to Adeno-Associated Virus Gene Delivery Vectors: The Race Between Clearance, Tolerance, Neutralization, and Escape. Annu. Rev. Virol. *4*, 511–534. https://doi.org/10.1146/annurev-virology-101416-041936.

44. Kaplitt, M.G., Feigin, A., Tang, C., Fitzsimons, H.L., Mattis, P., Lawlor, P.A., Bland, R.J., Young, D., Strybing, K., Eidelberg, D., and During, M.J. (2007). Safety and tolerability of gene therapy with an adeno-associated virus (AAV) borne GAD gene for Parkinson's disease: an open label, phase I trial. Lancet *369*, 2097–2105. https://doi.org/10.1016/S0140-6736(07)60982-9.

45. Maguire, A.M., High, K.A., Auricchio, A., Wright, J.F., Pierce, E.A., Testa, F., Mingozzi, F., Bennicelli, J.L., Ying, G.S., Rossi, S., et al. (2009). Age-dependent effects of RPE65 gene therapy for Leber's congenital amaurosis: a phase 1 dose-escalation trial. Lancet *374*, 1597–1605. https://doi.org/10.1016/S0140-6736(09)61836-5.

46. Bennett, J., Ashtari, M., Wellman, J., Marshall, K.A., Cyckowski, L.L., Chung, D.C., McCague, S., Pierce, E.A., Chen, Y., Bennicelli, J.L., et al. (2012). AAV2 gene therapy readministration in three adults with congenital blindness. Sci. Transl. Med. *4*, 120ra15. https://doi.org/10.1126/scitranslmed.3002865.

47. Varin, J., Morival, C., Maillard, N., Adjali, O., and Cronin, T. (2021). Risk Mitigation of Immunogenicity: A Key to Personalized Retinal Gene Therapy. Int. J. Mol. Sci. *22*, 12818. https://doi.org/10.3390/ijms222312818.

48. Shinohara, Y., Konno, A., Nitta, K., Matsuzaki, Y., Yasui, H., Suwa, J., Hiromura, K., and Hirai, H. (2019). Effects of Neutralizing Antibody Production on AAV-PHP.B-Mediated Transduction of the Mouse Central Nervous System. Mol. Neurobiol. *56*, 4203–4214. https://doi.org/10.1007/s12035-018-1366-4.

49. Klamroth, R., Hayes, G., Andreeva, T., Gregg, K., Suzuki, T., Mitha, I.H., Hardesty, B., Shima, M., Pollock, T., Slev, P., et al. (2022). Global Seroprevalence of Pre-existing Immunity Against AAV5 and Other AAV Serotypes in People with Hemophilia A. Hum. Gene Ther. *33*, 432–441. https://doi.org/10.1089/hum.2021.287.

50. Boutin, S., Monteilhet, V., Veron, P., Leborgne, C., Benveniste, O., Montus, M.F., and Masurier, C. (2010). Prevalence of serum IgG and neutralizing factors against adeno-associated virus (AAV) types 1, 2, 5, 6, 8, and 9 in the healthy population: implications for gene therapy using AAV vectors. Hum. Gene Ther. *21*, 704–712. https://doi.org/10.1089/hum.2009.182.

51. Dalkara, D., Byrne, L.C., Klimczak, R.R., Visel, M., Yin, L., Merigan, W.H., Flannery, J.G., and Schaffer, D.V. (2013). In vivo-directed evolution of a new adeno-associated virus for therapeutic outer retinal gene delivery from the vitreous. Sci. Transl. Med. *5*, 189ra176. https://doi.org/10.1126/scitranslmed.3005708.5/189/189ra76.

52. Sabatino, D.E., Mingozzi, F., Hui, D.J., Chen, H., Colosi, P., Ertl, H.C.J., and High, K. A. (2005). Identification of mouse AAV capsid-specific CD8+ T cell epitopes. Mol. Ther. *12*, 1023–1033. https://doi.org/10.1016/j.ymthe.2005.09.009.

53. Totten, D.J., Booth, K.T.A., Mosier, K.M., Cumpston, E.C., Whitted, C., Okechuku, V., Koontz, N.A., and Nelson, R.F. (2023). Human cochlear diffusion from the cerebrospinal fluid space with gadolinium contrast. Mol. Ther. *31*, 2566–2569. https://doi.org/10.1016/j.ymthe.2023.08.001.

54. Costa-Verdera, H., Unzu, C., Valeri, E., Adriouch, S., González Aseguinolaza, G., Mingozzi, F., and Kajaste-Rudnitski, A. (2023). Understanding and tackling immune responses to AAV vectors. Hum. Gene Ther. *34*, 836–852. https://doi.org/10.1089/hum.2023.119.

55. Viberg, A., and Canlon, B. (2004). The guide to plotting a cochleogram. Hear. Res. *197*, 1–10. https://doi.org/10.1016/j.heares.2004.04.016.

56. Landegger, L.D., Vasilijic, S., Fujita, T., Soares, V.Y., Seist, R., Xu, L., and Stankovic, K.M. (2019). Cytokine Levels in Inner Ear Fluid of Young and Aged Mice as Molecular Biomarkers of Noise-Induced Hearing Loss. Front. Neurol. *10*, 977. https://doi.org/10.3389/fneur.2019.00977.

57. Salt, A.N., Kellner, C., and Hale, S. (2003). Contamination of perilymph sampled from the basal cochlear turn with cerebrospinal fluid. Hear. Res. *182*, 24–33. https://doi.org/10.1016/s0378-5955(03)00137-0.

58. Brown, D., Zingone, A., Yu, Y., Zhu, B., Candia, J., Cao, L., and Ryan, B.M. (2019). Relationship between Circulating Inflammation Proteins and Lung Cancer Diagnosis in the National Lung Screening Trial. Cancer Epidemiol. Biomarkers Prev. *28*, 110–118. https://doi.org/10.1158/1055-9965.EPI-18-0598.